Geofluids (2001) 1, 2–10

FT-IR measurements of petroleum fluid inclusions: methane, *n*-alkanes and carbon dioxide quantitative analysis

J. PIRONON[1], R. THIERY[2], M. AYT OUGOUGDAL[3], S. TEINTURIER[1], G. BEAUDOIN[3] AND F. WALGENWITZ[4]

[1]UMR G2R-CNRS, Université H. Poincaré, Vandœuvre-lès-Nancy, France; [2]UMR 6524, Université B. Pascal, Clermont-Ferrand, France; [3]MEDEF, Département de Géologie et de Génie Géologique, Université Laval, Québec, Canada; [4]CSTJF, TotalFinaElf, Pau, France.

ABSTRACT

A recent advancement in petroleum geochemistry is to model fossil oil composition using microthermometric and volumetric data acquired from individual fluid inclusion analysis. Fourier Transform Infrared (FT-IR) microspectroscopy can record compositional information related to gas (CH_4 and CO_2) and alkane contents of petroleum inclusions. In this study, a quantitative procedure for FT-IR microspectrometry has been developed to obtain, from individual fluid inclusions, mol percentage concentrations of methane, alkanes and carbon dioxide as constraints to thermodynamic modelling. A petroleum inclusion in a sample from the Québec City Promontory nappe area was used as a standard to record a reference spectrum of methane. The analytical procedure is based on the measurement of CH_4/alkane and CH_4/CO_2 band area ratios. CH_4/alkane infrared band area ratio is obtained after spectral subtraction of the reference methane spectrum. This area ratio, affected by absolute absorption intensities of methane, methyl and methylene, provides a molar CH_4/alkane ratio. Methyl/methylene ratio (CH_2/CH_3) ratio is obtained following procedures established in previous work. CO_2/CH_4 concentration ratio is estimated from relative absolute absorption intensities. Application to natural inclusions from different environments shows good correlation between FT-IR quantification and PIT (petroleum inclusion thermodynamic) modelling.

Key-words: carbon dioxide, infrared intensity, methane, microspectrometry, *n*-alkane, petroleum fluid inclusions, PIT

Received 21 May 2000; accepted 28 September 2000

Corresponding author: Jacques Pironon, UMR G2R-CNRS, Université H. Poincaré, BP 239, F-54506 Vandœuvre-lès-Nancy, France.
E-mail: jacques.pironon@g2r.uhp-nancy.fr. Tel: +33 3 83 91 38 20. Fax: +33 3 83 91 38 01.

Geofluids (2001) 1, 2–10

INTRODUCTION

Petroleum inclusions are common in petroleum reservoirs and may be considered as fossil oils, which have preserved the original oil composition. Petroleum inclusion composition and phase equilibrium are related to the PVTX conditions at the time of trapping. Phase equilibrium data, such as homogenization temperature, obtained by microthermometry, and volumetric estimate of the gas/oil ratio, obtained by confocal scanning laser microscopy (CSLM), are the only data currently required to constrain thermodynamic models [VTFlinc, petroleum inclusion thermodynamic (PIT)] applied to petroleum inclusions (Aplin *et al.* 1999; Thiéry *et al.* 2000). Bulk methods such as gas chromatography–mass spectrometry (GC–MS) (Bratus *et al.* 1975; Horsfield & McLimans 1984; George *et al.* 1997), high-performance liquid chromatography (HPLC) (Pang *et al.* 1998) and nuclear magnetic resonance (NMR) (Dereppe *et al.* 1994) can provide bulk compositions of petroleum inclusions. However, these techniques may provide incorrect compositions if the sample contains multiple generations of oil inclusions, trapped in a single diagenetic mineral.

Analysis of individual inclusions is possible using molecular spectroscopies: visible Raman microspectroscopy can be applied in the case of nonfluorescent inclusions (Pironon 1993). Near-infrared FT-Raman can be applied in the case of weakly fluorescent inclusions but is still affected by fluorescence for most inclusions (Pironon *et al.* 1991). Fourier Transform Infrared (FT-IR) is the most powerful molecular microspectroscopic technique for analysing oil inclusions

(Barrès *et al.* 1987; Guilhaumou *et al.* 1990; Wopenka *et al.* 1990; Pironon *et al.* 1991). Recent development of laser micropyrolysis coupled with GC-MS also offers the potential for chemical characterization of individual inclusions (Greenwood et al. 1998). All of these techniques, whilst useful in a qualitative sense, have severe limitations that frequently prevent a quantitative approach. Limitations in FT-IR spectrometry can be minimized using synchrotron excitation (Guilhaumou *et al.* 1999), but this cannot be considered a routine technique applied to the characterization of petroleum inclusions. Synchrotron sources are not always available; analyses are time- and money-consuming.

The objective of this work is to decipher quantitative chemical information from conventional infrared spectra to constrain petroleum modelling. An analytical procedure will be defined and applied to reference inclusions. Results from FT-IR quantification will be compared with the results obtained from compositional modelling of these same inclusions. Quantification has been focused on methane, alkane and CO_2 concentrations by the analysis of the CH and CO stretching vibrations.

EQUIPMENT

The LEM laboratory (ENSG - Vandœuvre-lès-Nancy, France) uses a Bruker IFS 55 Fourier transform spectrometer, coupled with a Bruker microscope, which collects the infrared beam with cassegrain objectives ($\times$ 15 or $\times$ 36). Analysis of petroleum inclusions in thin (i.e. less than 300 μm) doubly polished sections is done by transmission, using a circular or a knife-edge diaphragm with a variable diameter aperture (> 8 μm). Spectral resolution is 4 cm^{-1}, and integration time is longer than 2 min and increases as the inclusion size decreases. Spectra are plotted in absorbance units in the mid-infrared range. The analytical limit is 2000 cm^{-1} for inclusions in quartz and 800 cm^{-1} for inclusions in fluorite owing to absorption by the host mineral. Spectra of atmospheric CO_2 and H_2O vapours are subtracted. The atmospheric CO_2 spectrum shows a band doublet at 2360 and 2339 cm^{-1} clearly different from the single-band infrared spectra of CO_2 under pressure or dissolved in oil. For each measurement, a reference spectrum is recorded in air or in an inclusion-free area of the host mineral. A Linkam microthermometric stage is coupled to the infrared microscope to record FT-IR spectra between – 180°C and + 600°C. We use BaF_2 windows, which are transparent in the mid-infrared range. Each spectrum is processed using the OPUS program (®Bruker). Band areas of CH and CO stretching bands are calculated. Bands with intensity higher than 1.3 are not taken into account because of mercury cadmium telluride (MCT) detector saturation.

Microthermometric measurements (homogenization and melting temperatures) have been acquired with a Chaix-meca stage (Poty *et al.* 1976) on a conventional optical microscope.

Gas/oil volumetric ratios have been measured with BioRad 1024 and Olympus Fluoview confocal scanning laser microscopes following procedure determined by Pironon *et al.* (1998). Volume of fluorescent liquid oil is measured at room temperature by CSLM whereas the volume of the gas bubble is approximated to a sphere and calculated from its diameter, which is measured by conventional transmission optical microscopy.

SAMPLES

Twelve different inclusions, taken from seven samples from different settings, were selected for application of the FT-IR quantitative analysis.

Two samples of petroleum inclusion-rich fluorite were analysed:

(1) An inclusion from the Cave-in-Rock fluorite-Pb-Zn district, southern Illinois, USA, described by Roedder (1984) and Pironon *et al.* (1998). It is a two-phase yellow oil inclusion with a homogenization temperature to the liquid phase at 112.6 ($\pm$ 0.1)°C. The gas volume percentage at 25°C is 9($\pm$ 0.5)%. This primary oil inclusion is associated with aqueous inclusions rich in CO_2 and CH_4, detected by Raman microspectrometry (Dubessy *et al.* 2000), homogenizing to the liquid phase between 140 and 146°C.

(2) A spherical petroleum inclusion from Boujabeur (Jebel Guebli-South of Tunis), described by Bouhlel *et al.* (1988) and Guilhaumou *et al.* (1988). It is a multiphase inclusion, with a gas volume of 9.5% at 25°C and a homogenization temperature to the liquid phase of 110.1°C. The inclusions contain several solid phases (i.e. anhydrite and 'organic' solids) attached to the inclusion wall in equal proportion for all inclusions. These organic solids could originate from post-trapping precipitation of aromatic fraction of the oil. Consequently, they should not interfere with FT-IR procedure and PIT modelling, which only take into account the aliphatic fraction of the oil. Associated aqueous inclusions have Th ranging from 110 to 140°C and salinities between 15 and 17 wt % NaCl equivalent.

Five samples of petroleum inclusion-rich quartz were selected:

(3) Eight inclusions from four different boreholes of the North Sea basin have been analysed. Seven were collected at a depth between 3400 and 3700 m in the Brent formation for Alwyn area. They are located in healed microfractures inside the detrital quartz grains. Inclusion 3a has a guitar-like shape, is 45 μm long, and homogenizes at 81.6°C to the liquid phase. The gas phase volume is 21.8% at room temperature. Inclusion 3b has an irregular shape with a length of 80 μm. The gas volume is 25% at 25°C and it homogenizes at a temperature of 94.7°C. Inclusion 3c has a simple parallelepiped shape, a size of 25 μm along the main axis, a low gas volume of 6.3% at 25°C and a homogenization temperature of 86.1°C. Inclusion 3d has a triangular shape, 15 μm length

size. It has a weak gas volume fraction at 25°C (3.1%) and a low homogenization temperature (68.7°C). Inclusion 3e has an ellipsoid shape, a length of 8 μm, a gas volume of 9% at 25°C and a homogenization temperature of 79.4°C. Inclusion 3f has an irregular shape and a length of 40 μm. The gas volume is 5.8% at room temperature and it homogenizes at 74.6°C. Inclusion 3g has an irregular shape, a length of 25 μm, a gas volume of 5.8% at 25°C and a homogenization temperature of 99.7°C. These petroleum inclusions are associated with aqueous inclusions homogenizing between 105 and 115°C.

The inclusion from Haltenbanken area belongs to the sandstones of the Garn formation cored at 3700 m. This inclusion is located inside quartz overgrowth and has an irregular shape with terminal thin channels. The gas volume is 80% at 25°C and it homogenizes at 121°C in gaseous phase. L + L + G → L + G transition at low temperature occurs at − 53°C. This inclusion is not associated with aqueous inclusion but it contains a small amount of water wetting the inclusion wall.

(4) Two negative crystal-shaped inclusions (Q21 and 5) within euhedral quartz in quartz-calcite-bitumen fractures from the Québec City Promontory nappe (Cambrian to Ordovician). The homogenization of inclusion Q21 is to the liquid phase near 54°C, and inclusion 5 is by critical behaviour at 33°C. The gas volume of Q21 and 5 at room temperature is near 40%. Similar inclusions have been described by Levine *et al.* (1991). At low temperature, a L + L + G → L + G transition occurs at − 68.6°C for inclusion 5 and at − 65°C for inclusion Q21. Rare associated aqueous inclusions have salinities close to 10 wt % NaCl equivalent and Th near 85°C.

ANALYTICAL PROCEDURE

The FT-IR analytical procedure involves three steps: recording of a methane reference spectrum; methane, alkane and CO_2 spectral area measurement in the unknown inclusion; and calibration of the quantitative FT-IR approach.

Methane reference spectrum

A 200-μm long inclusion from Québec City area (Q21) was chosen for FT-IR analysis focusing the infrared beam into the vapour phase (Fig. 1). The vapour phase is in contact with the inclusion wall, such that the FT-IR analysis does not take into account the liquid phase of the inclusion. FT-IR measurements were done at low temperatures before (Fig. 1A,B) and after (Fig. 1D) a (L + S) + L + V → (L + S) + V transition observed at − 65°C when liquid (L) and vapour (V) phases homogenize at critical state (Fig. 1C). Such partial miscibility at cryogenic state corresponds to a condensate gas behaviour (methane dominant with alkanes) (Luks *et al.* 1983). At − 167°C, the FT-IR spectrum of the gas phase shows the presence of methane, with its P, Q and R narrow branches, corresponding to gas at low pressure (near atmo-

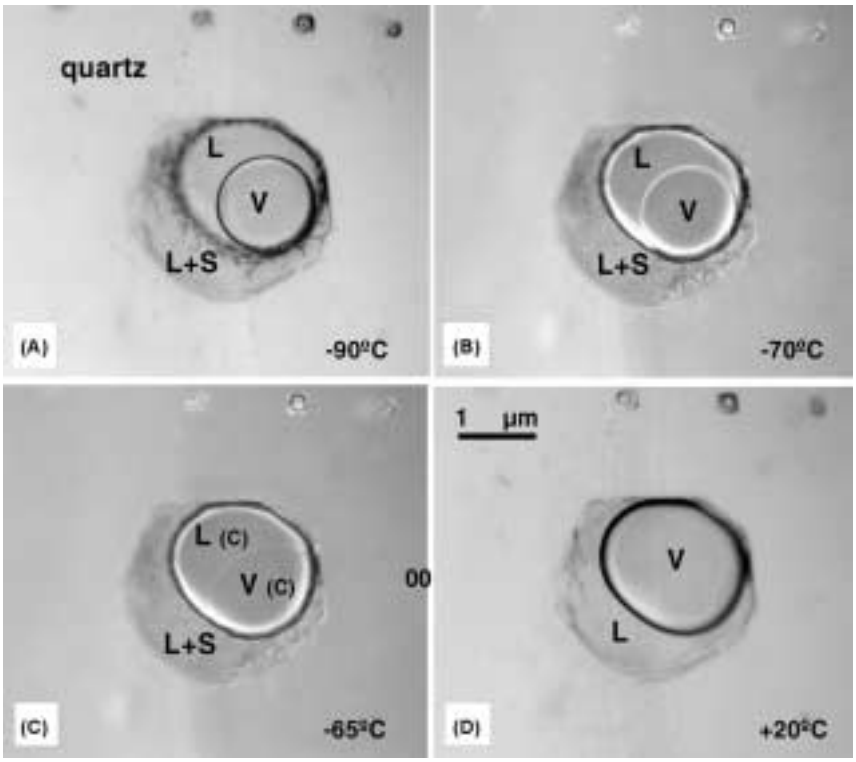

Fig. 1. Photomicrographs of inclusion Q21 from the Québec Promontory nappe at different temperatures, showing the (L + S) + L + V → L + V transition. L, liquid; S, solid; V, vapour; L(C), liquid near critical state; V(C), vapour near critical state.

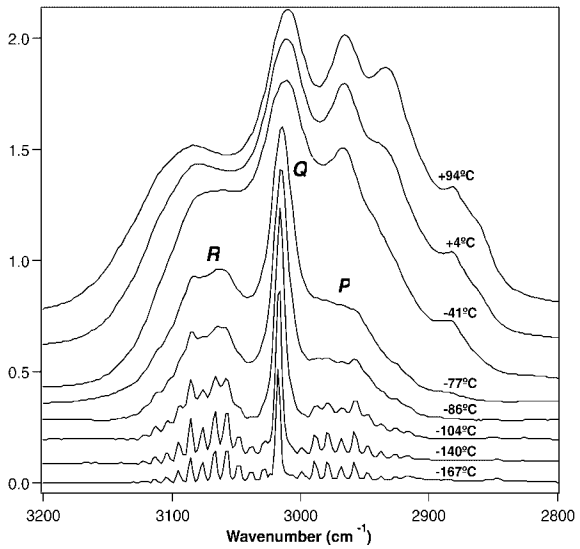

Fig. 2. FT-IR spectra of the gas phase of the Q21 inclusion from the Québec City Promontory nappe, recorded at different temperatures.

spheric pressure) (Herzberg 1968). CO_2 has disappeared from the vapour phase to be concentrated in the liquid phases. With increasing temperature, the bands become broader, indicating an increase of internal pressure (Fig. 2), and CO_2 partially migrates from liquid phases to the vapour phase. The full width at half maximum (FWHM) of the Q branch of methane rapidly increases up to the L + L + V → L + V transition at − 65°C, followed by a slow increase up to 100°C (Figs 2,3A). The peak position decreases from 3018 to 3010 cm^{-1} and from − 167 to − 50°C and seems to remain constant at high temperatures (Fig. 3B). Small peak position oscillations between 3010 and 3012 cm^{-1} are due probably to the 4 cm^{-1} spectral resolution of the FT-IR microspectroscope. It appears that methane spectrum is affected by pressure only near atmospheric conditions, which are attained in the inclusion at low temperature. At higher pressure, the methane spectrum has constant FWHM and peak position such that the Québec inclusion spectrum, recorded at room conditions, can be used as a reference.

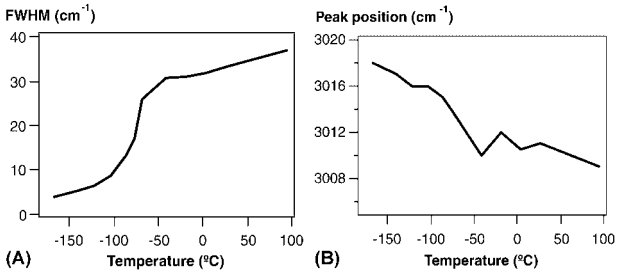

Fig. 3. Evolution of the full width at half maximum (FWHM) and of the position of the Q branch of methane for different temperatures. FT-IR spectra are recorded on the vapour phase of the Q21 inclusion from the Québec City Promontory nappe.

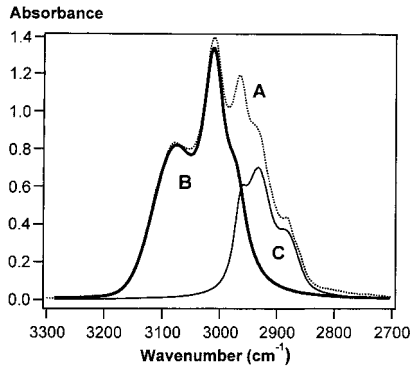

Fig. 4. FT-IR spectrum of methane (B) obtained after decomposition of the FT-IR spectrum of the gas phase (A) of the Q21 inclusion from the Québec City Promontory nappe. Spectrum C corresponds to the presence of alkane.

Nevertheless, the FT-IR spectrum is affected by alkane absorbance. With increasing temperature, methane-alkane partitioning between the gas and liquid phases in the L + V domain varies. Alkane concentration increases in the gas phase and its contribution must be subtracted from the methane peak. The methane spectrum was decomposed in seven main contributions using the Opus software: the three P, Q, R branches of CH_4, and four symmetric and asymmetric CH_2 and CH_3 bands (Fig. 4). The remaining methane reference spectrum is similar to the FT-IR spectrum of pure methane inclusion described by Barrès *et al.* (1987), and was used for the quantitative studies.

This standard inclusion has been preferred to pure CH_4 natural or synthetic inclusion to give a FT-IR spectrum as similar as possible to the spectrum of methane in petroleum basin conditions. Pure CH_4 inclusions are created in different P, T, X conditions than oil inclusions. It is suspected that such differences are marked on the FT-IR spectrum, by shift of the wavenumber of the maximum of intensity and by modification of the relative intensity of the P, Q, R branches of the stretching band of methane.

Methane, alkane and CO_2 spectral area measurement

Spectral procedure for the quantification of methane, alkane and CO_2 in petroleum inclusions consists of:

(1) recording the whole inclusion FT-IR spectrum at 25°C;
(2) baseline subtraction, including removal of the water contribution;
(3) atmospheric CO_2 infrared spectrum subtraction;
(4) integration of the methane + alkane contribution between 3200 and 2800 cm^{-1} (A_X), and of CO_2 (A_{CO_2});
(5) methane subtraction from the reference Q21 methane spectrum;
(6) area calculation of the remaining 3200–2800 cm^{-1} range (A_{alk}), and of the CH_2/CH_3 area ratio following Pironon & Barrès (1990); and

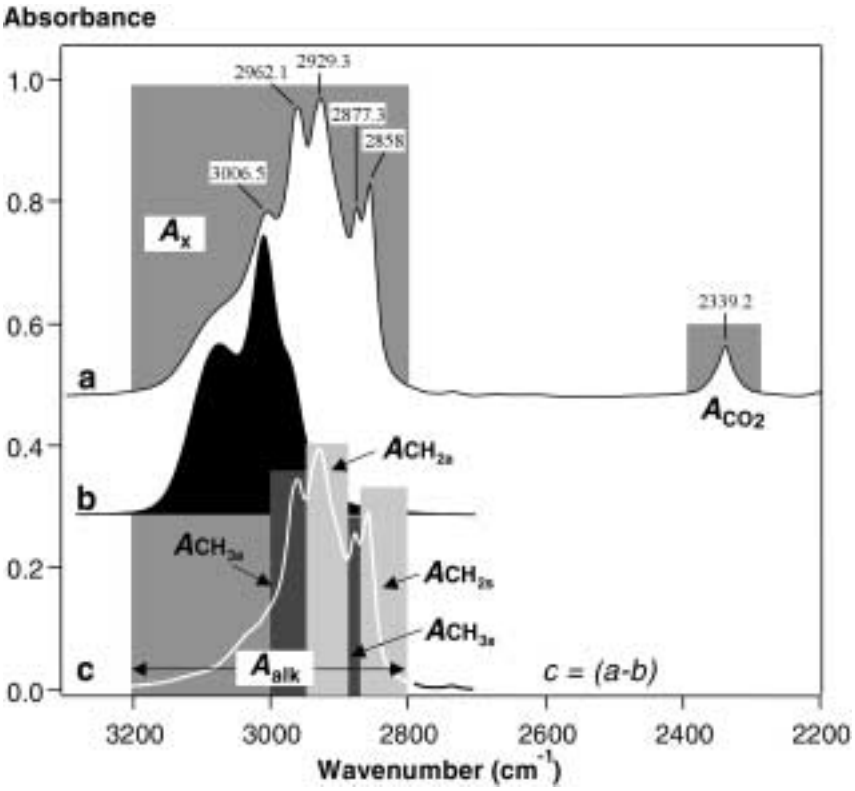

Fig. 5. Spectral procedure for the quantification of methane, alkane and CO_2 in petroleum inclusions. (A) FT-IR spectrum of the bulk inclusion; (B) reference spectrum of methane; (C) (a-b) spectrum subtraction. 7 spectrum areas are calculated: $[A_x]$, $[A_{CO_2}]$, $[A_{alk}]$, $[A_{CH_{3a}}]$, $[A_{CH_{2a}}]$, $[A_{CH_{3s}}]$, $[A_{CH_{2s}}]$.

(7) calculation of the methane area (A_{CH_4}) by ($A_X - A_{alk}$) subtraction.

Steps 4–7 are summarized Fig. 5.

Calibration of quantitative FT-IR

Different authors have measured infrared intensities of methane, alkanes and CO_2. Bode *et al.* (1980) and Gussoni (1982) have proposed absolute absorption intensities of 65.5 and 67 km mol^{-1} respectively for methane. Gribov (1964) and Riley *et al.* (1982) give an absolute absorption intensity for CO_2 of 610 km mol^{-1}. Kondo & Saëki (1973) give a value of 178 km mol^{-1} for ethane and 192 km mol^{-1} for propane. Jones & Sandorfy (1956) and Finkel (1966) show that absolute absorption intensities of alkanes increase with carbon number. From their observations, absorption values of 89 km mol^{-1} for the methyl group and of 63 km mol^{-1} for the methylene group can be used.

Beer-Lambert's law can be applied to our quantitative infrared measurement. The methane/alkane area ratio is related to the methane/alkane molar ratio by the following equation:

$$\frac{A_{CH_4}}{A_{alk}} = \frac{\varepsilon_1 \cdot [CH_4] \cdot e}{\varepsilon_2 \cdot [alk] \cdot e} \quad (1)$$

where A_{CH_4} and A_{alk} are the area of methane and alkane calculated from FT-IR spectrum, ε_1 and ε_2 are the absolute absorption intensities of methane and alkane, respectively, $[CH_4]$ and $[alk]$ are the molar concentrations of methane and alkane and e is the thickness of the inclusion.

Absolute absorption intensity of alkanes varies with carbon number and can be expressed by equation 2, where CH_2/CH_3 is the methylene/methyl ratio determined from the FT-IR spectrum.

$$\varepsilon_2 = 178 + 126\frac{CH_2}{CH_3} \quad (2)$$

Considering a binary system, composed of only methane and alkanes, and an absolute absorption intensity of 67 km mol^{-1} for methane, equation 1 becomes:

$$\frac{A_{CH_4}}{A_{alk}} = \frac{67 \cdot [CH_4]}{\left(178 + 126\frac{CH_2}{CH_3}\right) \cdot (100 - [CH_4])} \quad (3)$$

After development, equation 3 leads to the methane mol percentage of the petroleum inclusion by equation 4:

$$[CH_4] = \frac{100 \cdot A_{CH_4}\left(178 + 126\frac{CH_2}{CH_3}\right)}{67.A_{alk} + A_{CH_4}\left(178 + 126\frac{CH_2}{CH_3}\right)} \quad (4)$$

Figure 6 shows the influence of the CH_2/CH_3 ratio on the methane mol percentage calculation for binary systems. FT-IR methane quantification is very sensitive to CH_2/CH_3 ratio for high methane concentration and to small

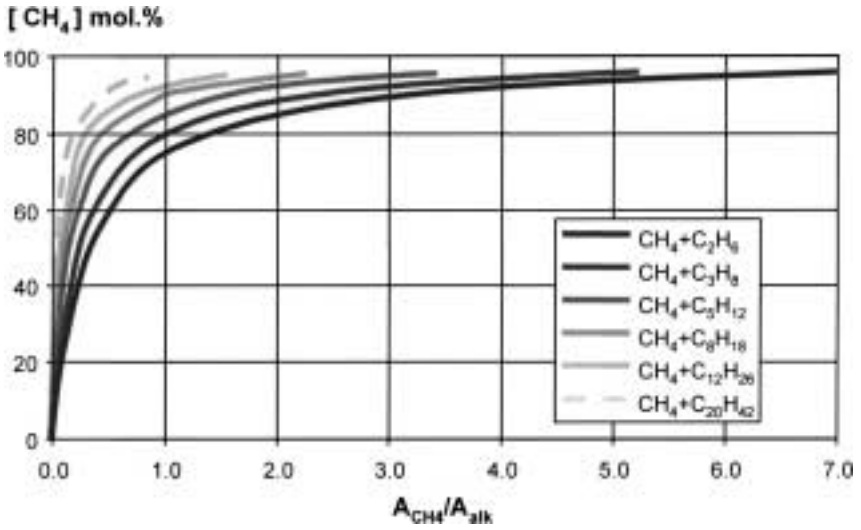

Fig. 6. Relations between measured infrared band area and methane concentration for some binary methane-alkane mixtures.

CH_4/alkane area ratio variations at low methane concentration.

Concentration of CO_2, in mol percentage, will be calculated from the methane concentration, taking into account their relative absolute absorption intensities (equations 5 and 6).

$$\frac{A_{CO_2}}{A_{CH_4}} = \frac{\varepsilon_3 \cdot [CO_2] \cdot e}{\varepsilon_1 \cdot [CH_4] \cdot e} \quad (5)$$

$$[CO_2] = \frac{67 \cdot [CH_4] \cdot A_{CO_2}}{610 \cdot A_{CH_4}} \quad (6)$$

Concentrations of methane, alkanes and CO_2 are therefore recalculated at 100 and given in mol percentage.

RESULTS AND DISCUSSION

Results of quantitative FT-IR analysis of six natural petroleum inclusions are summarized in Table 1. For each sample maximum and minimum values for CH_2/CH_3, $[CH_4]$, $[CO_2]$ and [Alk] parameters are reported because of the uncertainties of the CH_2/CH_3 measurement. The presence of a brine film around the oil phase inside an inclusion can create spectral deformations (pseudosaturation effect), modifying infrared intensities of the alkane contribution (Pironon & Barrès 1990, 1992). During routine FT-IR analysis of liquids in cells, quantification is limited by the difference between the refractive indices of the liquid and the window of the cell. It is recommended to regard with caution the results when refractive indices differ by more than 0.15 (Bertie & Apelblat 1996). A fluid inclusion can be approximated as a liquid in a cell. Effects of brine and of refractive index are frequently more intense for oil trapped in NaCl or CaF_2 than in quartz, because the refractive indices of quartz and natural oils are more or less similar. The pseudosaturation effect on FT-IR quantification decreases the alkane contribution in most cases [this effect could be observed on methane contribution only if methane contribution was higher than alkane

Table 1 CH_2/CH_3, $[CH_4]$, $[CO_2]$, [Alk] parameters acquired by FT-IR measurements for 11 inclusions trapped in fluorite (1, Illinois; 2, Tunisia) and Quartz (3, Alwyn; 4, Haltenbanken; 5, Québec). Parameters with * are calculated from PIT software, using Th, gas vol. %, and CO_2 approximation.

No. inclusion	1	2	3a	3b	3c	3d	3e	3f	3g	4	5
CH_2/CH_3 no. 1	2.4	3	1.7	1.9	2.3	1.8	1.8	2.1	1.7	2	2
CH_2/CH_3no. 2	4.3	6.1	2.1	2.6	3.8	2.3	2.4	3.2	2.1	2.9	3
$[CH_4]$ no. 1 (mol %)	26.3	15.1	48.6	44.3	13.2	23.8	29	24.7	17.3	62.7	60.9
$[CH_4]$ no. 2 (mol %)	33.9	21.6	51.6	49	17.5	26.4	32	30.4	19.1	68.2	66.7
$[CO_2]$ no. 1 (mol %)	5.3	11	1.9	1.3	4.1	0.6	-	0.2	0.7	4.3	1.2
$[CO_2]$ no. 2 (mol %)	6.8	15.7	2	1.5	5.4	0.7	–	0.3	0.8	4.7	1.3
[Alk] no. 1 (mol %)	68.4	73.9	49.6	54.4	82.7	75.6	71	75.3	82.7	37.3	37.9
[Alk] no. 2 (mol %)	59.3	62.7	46.5	49.5	77.1	72.9	68	69.6	80.9	31.8	32
$[CH_4]$ (mol %) PIT*	18 ± 5	16 ± 5	48 ± 5	47 ± 5	14 ± 5	24 ± 5	36 ± 5	29 ± 5	20 ± 5	71 ± 5	71 ± 5
ρ bulk (g/cm^3)*	0.82	0.80	0.56	0.58	0.83	0.92	0.70	0.81	0.90	0.20	0.38
Th (°C)	112.6	110.1	81.6	94.7	86.1	68.7	79.4	74.6	99.7	121	33
Gas vol. %	9.0	9.5	21.8	25	6.3	3.1	9.0	5.8	5.8	80	40

contribution (i.e. [CH_4] > 80%)]. This effect is observed on the spectra from the two fluorite samples from Illinois and Tunisia, and therefore the highest alkane concentration is considered accurate (Table 1). For quartz samples, no or only a slight pseudosaturation effect is detected in the FT-IR spectra, such that the lower alkane value is considered accurate.

Although no standard petroleum inclusions, with a well-known composition, exist that can be used to validate FT-IR quantitative analysis and to provide measurement accuracy, PIT modelling provides good argument to support the application of FT-IR quantitative analysis to petroleum inclusions. Modelling is based on homogenization temperatures measured by microthermometry and on gas volume estimate at room temperature measured by CSLM. CO_2 concentration, estimated from FT-IR spectra, is taken into account for composition modelling. Data are given with an accuracy of 5%. A good correlation between PIT and FT-IR procedure is obtained (Fig. 7). The Illinois fluorite inclusion shows a higher concentration using FT-IR (Table 1, Fig. 7). This result confirms the limit of FT-IR quantification for inclusions having FT-IR spectra affected by intense pseudosaturation. Application of this procedure is not recommended where evidence of FT-IR spectral deformation is observed. The most important difference between FT-IR analysis and PIT modelling is observed for inclusion 3e in quartz. This is explained by the tiny size of the inclusion (8 μm), corresponding to the size limit for FT-IR spectroscopy. Such limitation causes the nondetection of CO_2.

A good correlation between gas volume at room conditions and methane concentration is observed (Fig. 8A). Such correlation is explained by preferential methane partition in the gas phase. Inclusion bulk densities, computed with PIT modelling (Table 1), display a good negative correlation with methane concentrations (Fig. 8B). Comparisons with proton NMR results can be made on Alwyn samples. Methane concentrations, varying from 24 to 41 mol %, have been deduced from NMR (Dereppe *et al.* 1994). Such variation is close to the variations observed from FT-IR analysis, ranging from 17 to 50 mol %.

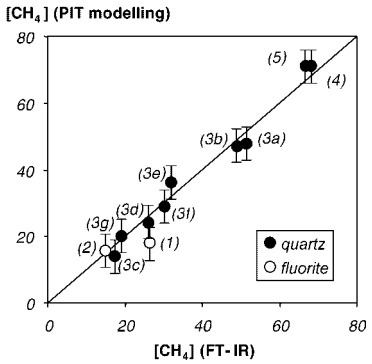

Fig. 7. Methane quantification (in mol percentage) by FT-IR and PIT modelling for 11 petroleum inclusions trapped in quartz and fluorite. See Table 1 for number correspondence.

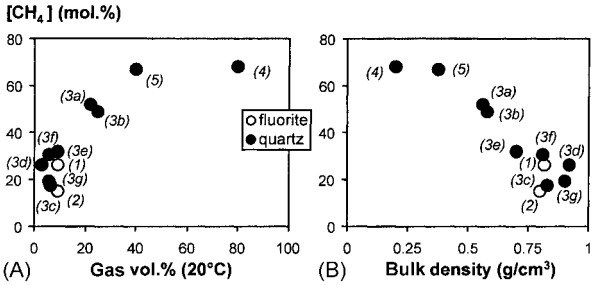

Fig. 8. Comparisons between methane concentration, determined by FT-IR quantification, and gas vol. % of the inclusion measured by CSLM at room temperature, and bulk density of the inclusion, determined by PIT modelling. See Table 1 for number correspondence.

Limits of FT-IR quantification can be classified in two groups: FT-IR intrinsic limitations; and limitations owing to the inclusion itself.

FT-IR intrinsic limitations

(1) Mid-infrared wavelengths preclude applications to inclusions smaller than 8 μm.
(2) Selection rules of molecular spectroscopy preclude the FT-IR analysis of strictly symmetric molecules such as molecular nitrogen.
(3) Absolute absorption intensity of H_2S is very low, such that this minor gas in petroleum inclusions cannot be detected.
(4) MCT detectors, used in FT-IR microscopy, have linearity in the C–H stretching range (2800–3200 cm^{-1}) limited to 1 or 1.3 in absorbance units. Large inclusions (more than 50 μm thick) will saturate the detector and the most intense bands of the FT-IR spectrum will be underestimated.

Limitations owing to the inclusions

(1) Absorption of the host mineral masks some infrared bands of the included oil. For instance, quartz absorption masks the aromatic C=C contributions, C=O and C–O groups, and CH bending vibrations; carbonate infrared absorption bands are superimposed on all bands of oil.
(2) When the thickness of the preparation increases, the signal/background ratio of the FT-IR spectrum decreases.
(3) The shape of the inclusion can create diffraction and refraction of the infrared beam, inducing interference fringes or baseline deformations that can be difficult to delete by spectral processing.

(4) Careful spectral subtraction of reference methane should avoid generation of negative absorbance values.
(5) Differences between refractive indices of host mineral and oil should be less than 0.15.
(6) Inclusions with high salinity aqueous liquid are not amenable to analysis because of interference between water film and oil phase. Salinity of the brine inside petroleum inclusion can be deduced from microthermometry of contemporaneous aqueous inclusions.
(7) The quantification procedure is not adapted for branched-alkanes-rich oils. CH groups interfere with CH_2 and CH_3 groups and perturb the CH_2/CH_3 estimate.
(8) Presence of CH aromatic groups can lead to the overestimate of methane.

FT-IR analysis of petroleum inclusions is the only analytical technique to obtain individual quantitative analysis of oil trapped in inclusions. Raman signal is masked by fluorescence, and bulk analyses (GC-MS, NMR) produce an average composition that cannot reproduce the heterogeneity encountered in one sample. For instance, inclusions 3b and 3c belong to the same fracture plane inside a detrital quartz grain from Alwyn. FT-IR and CSLM confirm the strong difference in methane concentration correlated with strong variations of volumetric properties. Such differences reveal variations of the petroleum reservoir evolution and give new insights about oil migration and trapping: loss of methane after unmixing, pressure regime variations, input of oils from different origins, and oil alteration.

FT-IR quantitative analysis is a useful tool to characterize petroleum inclusions. It is the only technique that can yield a CO_2 molar content. Quantitative FT-IR provides a good estimate of methane concentration, which is the main parameter that influences isopleth reconstruction. Isopleths limit the liquid and gas two-phase domain and provide the trapping pressure at the homogenization temperature in the case of methane-saturated oil. In addition, petroleum inclusion PVTX data enable calculation of the methane concentration of water phase in equilibrium with the oil. Difference or agreement between these concentrations, issued from calculation and results from methane analysis by Raman on aqueous inclusions (Dubessy *et al.* 2000), can help us to determine chronology between hydrocarbon and water inclusions.

CONCLUSIONS

PVTX characterization of petroleum inclusions is of strategic interest in the understanding of fluid migration. FT-IR quantitative analysis of methane, alkanes and CO_2 is feasible for individual inclusions, taking into account the limitations of this technique. The analytical procedure is based firstly on determination of a standard methane spectrum and secondly on quantification of the spectral area of methane, alkanes and CO_2 by the absolute absorption intensities. Applications to natural inclusions from a variety of environments show good agreement with the results of composition modelling. Coupled with microthermometry (homogenization temperatures of petroleum inclusions), CSLM (gas vol. %), thermodynamic modelling and Raman microscopy (methane concentration in aqueous inclusion), FT-IR quantitative analysis is well-adapted to determine methane and CO_2 content of petroleum inclusions coexisting with aqueous inclusions.

Results of FT-IR quantification of the oil in inclusions should give new insights on pressure and temperature of fluid migration and on petroleum evolution between genesis and present time. Such quantification procedure is well-adapted to 'conventional oils and gases' produced during oil and gas windows, but is not adapted to the analysis of oils rich in branched alkanes and/or aromatic rings. Fossil oil characterization should be further enhanced by biomarker analysis, such as aromatic and heteroatom compounds.

ACKNOWLEDGEMENTS

The authors wish to thank C. Laplace-Builhe from BioRad and J. L. Coupier from Olympus for their help with 3D image acquisition by confocal scanning laser microscopy.

REFERENCES

Aplin AC, Macleod G, Larter SR, Pedersen KS, Sorensen H, Booth T (1999) Combined use of confocal laser scanning microscopy and PVT simulation for estimating the composition and physical properties of petroleum in fluid inclusions. *Marine and Petroleum Geology*, **16**, 97–110.

Barrès O, Burneau A, Dubessy J, Pagel M (1987) Application of micro-FT-ir spectroscopy to individual hydrocarbon fluid inclusion analysis. *Applied Spectroscopy*, **41**, 1000–8.

Bertie JE, Apelblat Y (1996) Infrared intensities of liquids XIX: a simple and effective approximate method for the calculation of infrared optical constant spectra of liquids from transmission measurements. *Applied Spectroscopy*, **50**, 1039–46.

Bode JHG, Smit WMA, Visser T, Verkruijsse HD (1980) The absolute infrared intensities of propyne-d/sub 0/ and propyne-d/sub 3/. *Journal of Chemical Physics*, **72**, 6560–70.

Bouhlel S, Fortuné JP, Guilhaumou N, Touray JC (1988) Les minéralisations stratiformes à F-Ba de Hammam Zriba, Jebel Guébli (Tunisie nord orientale): l'apport des études d'inclusions fluides à la modélisation génétique. *Mineral Deposita*, **23**, 166–73.

Bratus MD, Svoren IM, Danysh VV (1975) Inclusions of hydrocarbons in 'Marmorosh diamonds' from Carpathians as indicators of migration of oil fluids. Carbon and its compounds in endogenic processes of mineral formation (Abstract). *COFFI*, **8**, 28.

Dereppe JM, Pironon J, Moreau C (1994) Characterization of the composition of fluid inclusion in minerals by ^{1}H NMR. *American Mineralogist*, **79**, 712–8.

Dubessy J, Buschaert S, Lamb W, Pironon J, Thiéry R (2000) Methane-bearing aqueous fluid inclusions: Raman analysis, thermodynamic modelling and application to petroleum basins. *Chemical Geology*, in press.

Finkel AG (1966) Experimental and theoretical study of absolute intensities in the infrared spectra of gaseous hydrocarbons. *Optometry and Spectroscopy*, **20**, 432–5.

George SC, Krieger FW, Eadington PJ, Quezada RA, Greenwood PF, Eisenberg LI, Hamilton PJ, Wilson MA (1997) Geochemical comparison of oil-bearing fluid inclusions and produced oil from the Toro sandstone, Papua New Guinea. *Organic Geochemistry*, **26**, 155–73.

Greenwood PF, George SC, Hall K (1998) Applications of laser micropyrolysis-gas chromatography-mass spectrometry. *Organic Geochemistry*, **29**, 1075–89.

Gribov LA (1964) *Intensity Theory for Infrared Spectra of Polyatomic Molecules* (English translation by P.P. Sutton), p. 106. Consultants Bureau, New York.

Guilhaumou N, Dumas P, Ingrin J, Carr GL, Williams GP (1999) Synchrotron infrared microspectrometry applied to petrography in micron scale range. *Internet Journal of Vibrational Spectroscopy*, **3**, 14.

Guilhaumou N, Szydlowskii N, Pradier B (1990) Characterization of hydrocarbon fluid inclusions by infrared and fluorescence microspectrometry. *Mineralogical Magazine*, **54**, 311–24.

Guilhaumou N, Touray JC, Bouhlel S (1988) Stretching of hydrocarbon fluid inclusions in fluorite at 200 and 400 bars confining pressure. Application to low-pressure geobarometry. *Bulletin Minéralogie*, **111**, 421–6.

Gussoni M (1982) Infrared intensities by parametric methods; a guided tour. In: *Vibrational Intensities in Infrared and Raman Spectroscopy* (eds Person WB, Zerbi G). Elsevier, Amsterdam.

Herzberg G (1968) *Molecular Spectra and Molecular Structure II. Infrared and Raman Spectra*. Van Nostrand Reinhold Company, New York.

Horsfield B, McLimans RK (1984) Geothermometry and geochemistry of aqueous and oil-bearing fluid inclusions from Fateh Field, Dubai. *Organic Geochemistry*, **6**, 733–40.

Jones RN, Sandorfy C (1956). *Chemical Applications of Spectroscopy IV Infrared and Raman Spectrometry: Applications*. Interscience, New York.

Kondo S, Saëki S (1973) Infrared absorption intensities of ethane and propane. *Spectrochimica Acta*, **29A**, 735–51.

Levine JR, Samson IM, Hesse R (1991) Occurrence of fracture-hosted impsonite and petroleum fluid inclusions, Quebec City Region, Canada. *AAPG Bulletin*, **75**, 139–55.

Luks KD, Merrill RC, Kohn JP (1983) Partial miscibility behavior in cryogenic natural gas systems. *Fluid Phase Equilibria*, **14**, 193–201.

Pang LSK, George SC, Quezada RA (1998) A study of the gross compositions of oil-bearing fluid inclusions using high performance liquid chromatography. *Organic Geochemistry*, **29**, 1149–61.

Pironon J (1993) Estimation de la longueur de chaîne des hydrocarbures des inclusions fluides par spectrométrie Raman. *Compte-Rendus de l'Académie des Sciences, Paris*, **316** Série II, 1075–82.

Pironon J, Barrès O (1990) Semi-quantitative FT-IR microanalysis limits: evidence from synthetic hydrocarbon fluid inclusions in sylvite. *Geochemica Cosmochemica Acta*, **54**, 509–18.

Pironon J, Barrès O (1992) Influence of brine-hydrocarbon interactions on FT-IR microspectroscopic analyses of intracrystalline liquid inclusions. *Geochemica Cosmochemica Acta*, **56**, 169–74.

Pironon J, Canals M, Dubessy J, Walgenwitz F, Laplace-Builhe C (1998) Volumetric reconstruction of individual oil inclusion by confocal scanning laser microscopy. *European Journal of Mineralogy*, **10**, 1143–50.

Pironon J, Sawatzki J, Dubessy J (1991) Nir FT-Raman microspectroscopy of fluid inclusions: comparisons with VIS Raman and FT-ir microspectroscopies. *Geochemica Cosmochemica Acta*, **55**, 3885–91.

Poty B, Leroy J, Jachimowicz L (1976) Un nouvel appareil pour la mesure des températures sous le microscope: l'installation de microthermométrie Chaixmeca. *Bulletin de la Société Française de Minéralogie et Cristallographie*, **99**, 182–6.

Riley G, Susuki S, Orville-Thomas WJ (1982) Dipole moment parameters and infrared band intensities. In: *Vibrational Intensities in Infrared and Raman Spectroscopy* (eds Person WB, Zerbi G). Elsevier, Amsterdam.

Roedder E (1984) Fluid inclusions. *Reviews in Mineralogy*, **12** (ed. Ribbe PH). Mineralogical Society of America.

Thiéry R, Pironon J, Walgenwitz F, Montel F (2000) PIT (Petroleum Inclusion Thermodynamic): a new modelling tool for the characterisation of hydrocarbon fluid inclusions from volumetric and microthermometric measurements. *Journal of Geochemical Exploration*, **69–70**, 701–4.

Wopenka B, Pasteris JD, Freeman. JJ (1990) Analysis of individual fluid inclusions by Fourier transform infrared and Raman microspectroscopy. *Geochemica Cosmochemica Acta* **54**, 519–33.